

# The Numerical Analysis of Reinforced Concrete Beams Using Embedded Discontinuities

R. Costa<sup>1</sup>, J. Alfaiate<sup>2</sup>

**Abstract:** In this paper a numerical simulation is performed on the behaviour of reinforced concrete beams, submitted to initial damage, subsequently strengthened with external steel plates bonded with epoxy. Modelling these structures requires the characterization of the behaviour of different materials as well as the connection between them. Fracture is modelled within the scope of a discrete crack approach, using a formulation in which strong discontinuities are embedded in the finite elements. In this approach, the displacement field is truly discontinuous and the jumps are non-homogeneous within each parent element [Alfaiate, Wells and Sluys (2000)].

**keyword:** Strong discontinuities, Reinforced concrete, External reinforcement, Bond-slip.

## 1 Introduction

The strengthening and repair technique using glued steel plates, in parallel with other techniques of reinforcement with non-metallic materials, has been frequently applied to beams, as well as to slabs and columns. In this paper the behaviour of reinforced concrete beams is studied; these beams were first submitted to initial damage and subsequently repaired and strengthened with external steel plates bonded with epoxy.

The modelling of these structures requires the characterization of the behaviour of different materials as well as the connection between them. In the description of the concrete behaviour, two non-linear phenomena are central: i) cracking and ii) crushing.

In the past, cracking has been modelled according to two different approaches: the smeared crack approach and the discrete crack approach. In the smeared approach, the constitutive relations of the continuum are modified, in order to take into account softening under tensile stresses. The microcracks are smeared in a band,

usually corresponding to the width of one element. In this case it is possible to identify the cracked elements but not the crack paths, since cracking never localizes into a discontinuous surface. Mesh dependency is obtained unless special regularization procedures are introduced, which are introduced in nonlocal, strain gradient or rate dependent models.

In the discrete crack approach, cracking / microcracking is assumed to localize into a discontinuity surface, also called a fictitious crack, since stress transfer between its faces is still possible. In general, interface elements with initial zero width are used to simulate these discontinuities. The interface elements are aligned with the element boundaries and no mesh dependency is obtained with this approach. However, if the crack path is not known *a priori*, remeshing may be required, which usually leads to distorted meshes.

More recently, two major numerical approaches compete in simulating cracking without introducing any of the short-comings mentioned above: i) the extended finite element method [Duarte and Oden. (1996), Babuška and Melenk. (1997), Mões *et al.* (1999), Wells and Sluys (2000)] and ii) the strong embedded discontinuity approach [Dvorkin *et al.* (1990), Simo *et al.*(1993), Lotfi and Shing (1995), Armero and Garikipati (1996), Larsson and Runesson (1996), Oliver (1996a), Oliver (1996b), Jirásek and Zimmermann (2001a), Jirásek and Zimmermann (2001b)]. In the strong embedded discontinuity approach, cracking is embedded into the parent elements. In particular, Oliver and his co-workers introduced the Continuous Strong Discontinuous Approach, in which fracture emerges as a natural evolution of damage from the continuum to a localized discontinuity. However, although this approach is quite useful when the bulk behaviour is clearly non-linear, it is often the case that the non-linearities are mostly due to the fracture behaviour, the bulk behaviour remaining linear-elastic. As a consequence, the fracture model can be chosen independently from the bulk, in a pure discrete way. In

<sup>1</sup> ADEC, EST-UALg, Faro, Portugal

<sup>2</sup> ICIST and IST, Lisbon, Portugal



### 3 Numerical behaviour and implementation

In this work, a stress/displacement ( $\mathbf{t}$ - $\mathbf{w}$ ) relation is used for the embedded cracks, based on a local damage model [Alfaiate, Wells and Sluys (2000)]:

$$\mathbf{t} = (1 - d)\mathbf{T}_{el}\mathbf{w}, \quad (1)$$

in which,  $d$  is a damage variable ( $0 \leq d \leq 1$ ) and  $\mathbf{T}_{el}$  is the elastic constitutive tensor in which all the off-diagonal components are null and the diagonal components are penalty functions used to avoid overlapping of the faces of closed cracks. The damage evolution law is:

$$d = d(k) = 1 - \exp\left(-\frac{f_{t0}}{G_F}k\right), \quad (2)$$

where  $k$  is a scalar variable that corresponds to the maximum positive normal component of the displacements jump:

$$k = \max \langle w_n \rangle^+, \quad k \geq 0, \quad (3)$$

$f_{t0}$  is the initial traction resistance (taken equal to  $f_{ctm}$ ) and  $G_F$  is the fracture energy. A loading function  $f$  is also defined by:

$$f = w_n - k, \quad (4)$$

Mode-I fracture is assumed for cracking initiation.

Modelling of the reinforcements, both internal and external, was done with linear 2 node finite elements, adopting an elastoplastic constitutive relation. The internal reinforcement / concrete bond was modelled with interface elements overlaid on top of the concrete mesh, using the constitutive relation given by the CEB-FIP model code 90 [CEB (1991)]. The adhesion between external reinforcement and concrete was modelled by interface elements with zero initial thickness, introducing a constitutive relation, with exponential softening, relative to the Mode-II fracture. The parameters that characterize this connection are: i) the cohesion ( $c$ ), ii) the shear stiffness ( $K_{int}$ ) and the fracture energy in Mode-II,  $G_F^II$ . The adopted values were taken from a parametric study presented in [Neto and Alfaiate (2003)], where it was found that the exterior reinforcement-epoxy connection breaks normally by detaching a layer of concrete adjacent to the reinforcement.

The adopted values are: cohesion,  $c = 2.50$  MPa, shear stiffness,  $K_{int} = 10^3$  MPa/mm and the fracture energy in Mode II,  $G_F^II = 1.38$  N.mm/mm<sup>2</sup>.

The use of nonlinear constitutive relations requires, in general, the use of an iterative procedure. In this paper, a different method is introduced, based on a formulation presented in [Rots (2001)] for the continuum, called sequentially linear model. Here, as well as in [Alfaiate, Almeida and Gago (2003)], a new version of the sequentially linear model is used to describe the local behaviour of the fictitious cracks. In this model, the response of the structure is not obtained incrementally; instead, a total formulation is used, in which the stiffness of the structure is decreased according to a material model, obtaining successive equilibrium states through the use of successive linear analyses.

### 4 Variational formulation used for the finite elements with embedded cracks

In the discrete cracking approach using embedded cracks, whenever the principal tensile stress equals the concrete tensile strength ( $f_{ct}$ ) a discontinuity is embedded in the finite element. In this discontinuity four additional global nodes are inserted, two at each boundary of the element [Alfaiate, Wells and Sluys]. The total displacement values correspond to the addition of a continuous part,  $\hat{\mathbf{u}}$ , with a discontinuous part corresponding to the displacement jump  $[[\mathbf{u}]]$  in the discontinuity surface [Alfaiate, Simone and Sluys (2003)]:

$$\mathbf{u}(\mathbf{x}) = \hat{\mathbf{u}}(\mathbf{x}) + H_{\Gamma_d}[[\mathbf{u}]], \quad (5)$$

where  $H_{\Gamma_d}$  is defined as;

$$H_{\Gamma_d} = H_{\Gamma_d} - (1 - r), \quad 0 \leq r \leq 1, \quad (6)$$

and  $H_{\Gamma_d}$  is the Heaviside function. The variational formulation at the element level is obtained applying the principle of virtual work:

$$\begin{aligned} & - \int_{\Omega \setminus \Gamma_d} (\nabla^s \delta \hat{\mathbf{u}}) : \boldsymbol{\sigma}(\hat{\boldsymbol{\varepsilon}}) d\Omega + \int_{\Omega \setminus \Gamma_d} \delta u \cdot \mathbf{b} d\Omega \\ & + \int_{\Gamma_t} \delta u \cdot \bar{\mathbf{t}} d\Gamma + \int_{\Gamma_d} \delta [[u]] \cdot \mathbf{t}^+ d\Gamma = 0 \end{aligned} \quad (7)$$

where  $\mathbf{b}$  are the body forces,  $\mathbf{t}$  are the stresses acting on the boundary and the last integral represents the energy dissipated in the crack discontinuity  $\Gamma_d$ .

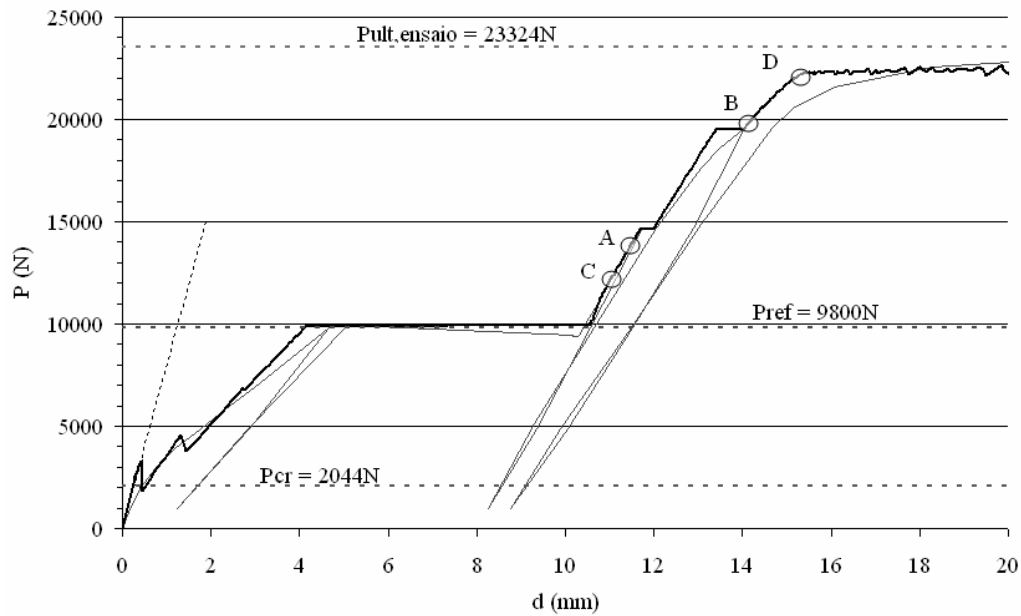


Figure 2 : P-Δ curves for beam type B with low level of initial damage

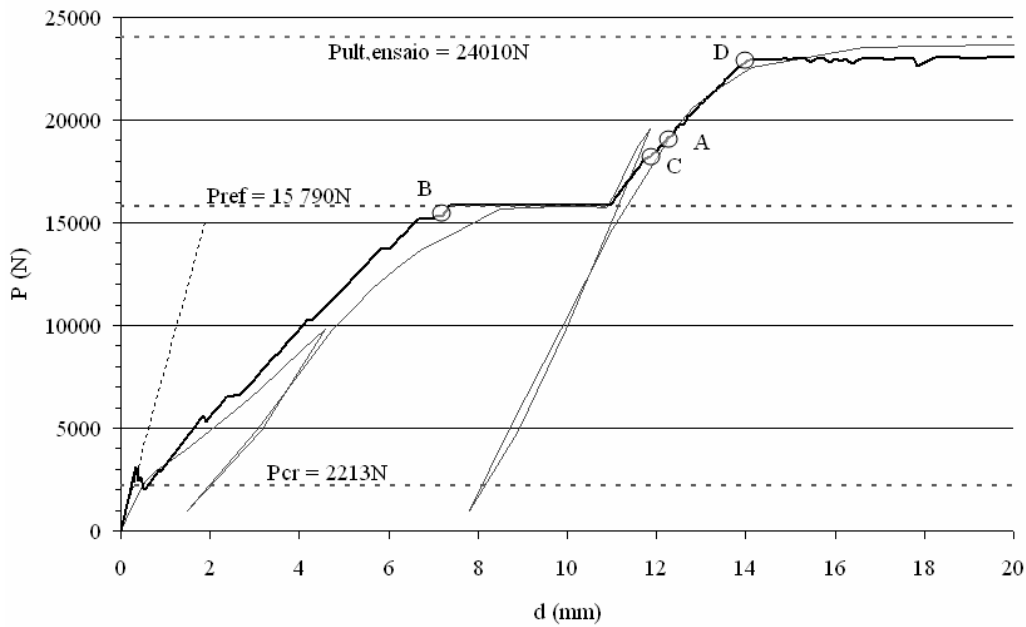


Figure 3 : P-Δ curves obtained with high level of initial damage

In equation (7) the stresses  $t$  in the discontinuity surface are obtained using the stress-jump law described in section 3.

### 5 Numerical results

In this section the numerical results are presented. First, the experimental (thin line) and numerical (thick line)

load-displacement curves obtained at mid-span are compared. The cracking load – ( $P_{cr}$ ) and the ultimate load ( $P_{ult}$ ) are marked in the graphics.

Two different damage levels were applied to the beams before reinforcement (see figs. 2 and 3). During the experimental tests, the loading was kept fixed for some days before repairing; due to the high level of previous dam-

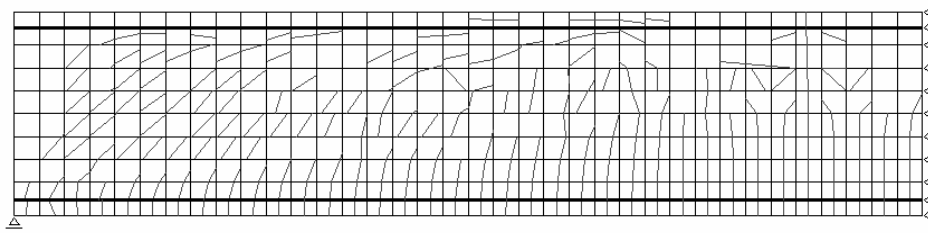


Figure 4 : Crack pattern obtained without micro crack filtering

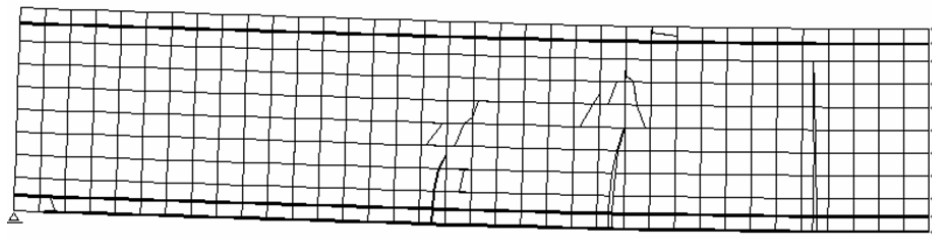


Figure 5 : Crack pattern over the deformed beam, obtained filtering cracks widths less than  $10\mu\text{m}$  (before strengthening)

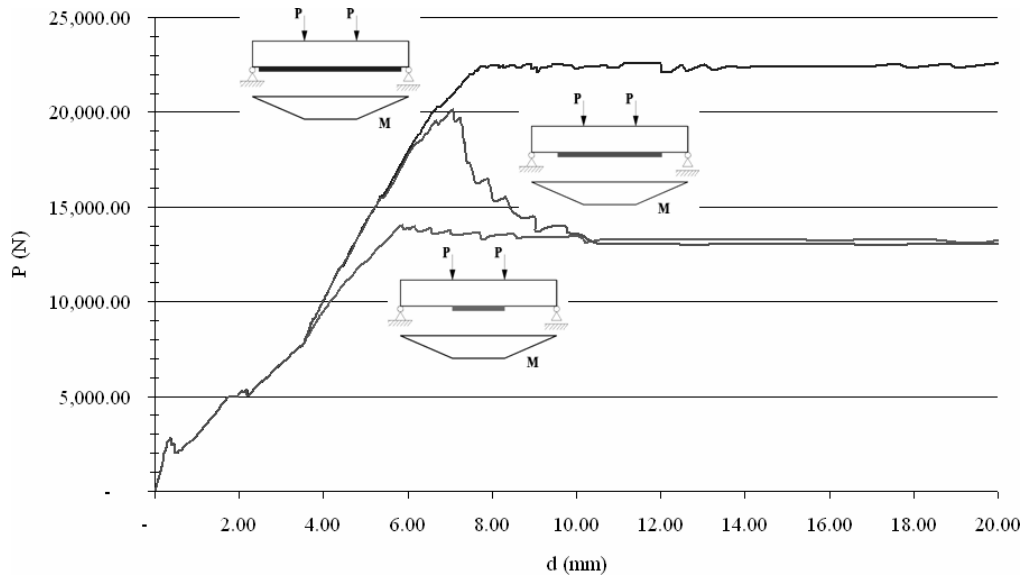


Figure 6 : Numerical test on bonding and plate length

age, creep took place, which was not modelled numerically; the corresponding additional displacements due to creep were added in the graphics to permit the comparison with the experimental results. The unloading cycles were not modelled numerically either.

In order to clarify the P- $\Delta$  graphics shown below, some noticeable points were marked on the numerical curves, namely:

- point A - identifies the load for which the stress  $f_{cm}$  was first attained;
- point B - beginning of internal reinforcement yield;
- point C - beginning of epoxy glue interface yielding;
- point D - beginning of external reinforcement (plate) yielding;

Analyzing the load-displacement graphics, it is possible to verify that a good approach between the numerical and experimental results is obtained. The differences found can be explained by: i) the influence of the unloading cycles, ii) the choice of the bond-slip relationship and iii) the lack of softening in the elastoplastic law adopted for the concrete under compression.

In figures 4 and 5 the cracking pattern under the ultimate load is presented which, in general, is similar to the one obtained experimentally. In figure 3, some of the cracks drawn correspond to micro cracks (fictitious). Notice that, due to the fact that each element is only able to present a single discontinuity, some of the cracks are not continuous. The crack pattern consists of vertical cracks at mid span and  $45^\circ$  cracks near the support, as expected.

In figure 5, the cracks widths are represented and micro cracks are filtered, allowing the identification of the main cracks in a clear way.

Some tests were carried out with similar beams using top anchorage with mechanical bolts. The results obtained both experimentally and numerically were similar to the results obtained without anchorage. Thus, it is concluded that, in this case, the anchorage length was enough and there was no failure of the glued connection.

In order to obtain conclusions on the importance of bonding in this type of structure, three numerical tests were made, changing both the bonded length and the plate length (see fig.6). When the plate covers the whole lower surface of the beam and the full strength of the plate is mobilized, an increase of both the stiffness and the ultimate load is obtained.

A strong decrease of the plate length (to the central zone length), gives rise to failure in the glue interface and a decrease of the ultimate load. An insufficient bonding length (a mean value of the previous ones) leads to a somewhat brittle solution: compared to the shorter bond length analyzed, stiffness is improved and a higher ultimate load is obtained. However, instead of a ductile rupture, a sudden drop in the load/displacement relationship occurs which can be dangerous, specially if the load is applied in fast manner. Similar results were obtained for beams with  $A_{sR} / A_{s1} = 1$ , as presented in [Costa (2005)].

## 6 Conclusions

In this paper, the finite element method is used to model externally strengthened beams with bonded steel plates.

Fracture in concrete is described by a discrete crack approach with an embedded technique. The behaviour of the connection between the internal reinforcement and the concrete is modelled using interface elements with null initial thickness and the constitutive relation given by the CEB-FIP MC90. The bonding of the steel plate with epoxy is described also using interface elements under mode-II fracture, using a model previously introduced in another work [Neto and Alfaiate (2003)].

It was shown that this approach leads to good results when compared to the experimental ones, namely the crack paths and the load-displacement curves. It was also numerically confirmed that, if the anchorage length is sufficient, the use of end mechanical anchors doesn't change the structural response.

## References

- Alfaiate, J.** (1986): O reforço por adição de elementos metálicos em vigas de betão armado submetidas à flexão simples, Dissertação de Mestrado, IST, Lisboa.
- Alfaiate, J.; Wells, G. N.; Sluys, L. J.** (2000): On the use of embedded discontinuity elements with crack path continuity for mode I and mixed mode fracture, *Engineering Fracture Mechanics*, 69 (6), pp. 661-686.
- Alfaiate, J.; de Almeida, J. R.; Gago, A.** (2003): On the numerical analysis of localized damage in masonry structures, in *Second International Conference on Structural Engineering and Construction*, ISEC-02, Roma.
- Alfaiate, J.; Simone, A.; Sluys, L.J.** (2003): Non-homogeneous displacement jumps in strong embedded discontinuities, *International Journal of Solids and Structures* 40.
- Armero, F.; Garikipati, K.** (1996): An analysis of strong discontinuities in multiplicative finite strain plasticity and their relation with the numerical simulation of strain localization. *International Journal for Numerical Methods in Engineering* 33 (20-22), pp. 2863-2885.
- Babuška, I.; Melenk, J. M.** (1997): The partition of unity method. *International Journal for Numerical Methods in Engineering* 40 (4), pp. 727-758.
- CEB – Comité Euro-International du Béton** (1990): CEB-FIP Model Code 1990, Thomas Telford, June (1991).
- Costa, R.** (2005): Modelação de vigas de betão armado reforçadas com chapas metálicas. Dissertação de

Mestrado, IST, Lisboa.

**de Borst, R.; Remmers, Joris J.; Needleman, A.; Abellan, M.** (2003): Discrete vs smeared crack models for concrete fracture: bridging the gap, in *Computational Modelling of Concrete Structures*, A.A. Balkema Publishers, pp. 3-16, Lisse.

**Duarte, C. A.; Oden, J. T.** (1996): H-p clouds – an h-p meshless method. *Numerical Methods for Partial Differential Equations* 12 (6), pp. 673-705.

**Dvorkin, E. N.; Cuitino, A. M.; Goia, G.** (1990): Finite elements with displacement interpolated embedded localization lines insensitive to mesh size and distortions. *International Journal for Numerical Methods in Engineering* 30, pp. 541-564.

**Jirásek, M.; Zimmermann, T.** (2001a): Embedded crack model: Part I. Basic formulation. *International Journal for Numerical Methods in Engineering* 50, pp. 1269-1290.

**Jirásek, M.; Zimmermann, T.** (2001b): Embedded crack model: Part II. Combination with smeared cracks. *International Journal for Numerical Methods in Engineering* 50, pp. 1291-1305.

**Larson, R.; Runesson, K.** (1996): Element-embedded localization band based on regularized displacement discontinuity. *ASCE Journal of Engineering Mechanics* 122 (5), pp. 402-411.

**Lilliu, G.; van Mier, J. G. M.** (2000): Simulation of 3D crack propagation with the lattice model, in *MaterialsWeek 2000*, <http://www.materialsweek.org/proceedings>, ed.

**Lotfi, H. R.; Shing, P. B.** (1995): Embedded representation of fracture in concrete with mixed finite elements. *International Journal for Numerical Methods in Engineering* 38 (8), pp. 1307-1325.

**Möes, N.; Dolbow, J.; Belytschko, T.** (1999): A finite element method for crack growth without remeshing. *International Journal for Numerical Methods in Engineering* 46 (1), pp. 131-150.

**Neto, P.; Alfaiate, J.; Pires, E. B. ; Almeida, J. R.** (2003): A influência do modo II de fractura no reforço do betão com FRP, ed. J. I. Barbosa, Évora, pp. 57-64.

**Oliver, J.** (1996a): Modelling strong discontinuities in solid mechanics via strain softening constitutive equations. Part 1: Fundamentals. *International Journal for Numerical Methods in Engineering* 39 (21), pp. 3575-

3600.

**Oliver, J.** (1996b): Modelling strong discontinuities in solid mechanics via strain softening constitutive equations. Part 2: Numerical simulation. *International Journal for Numerical Methods in Engineering* 39 (21), pp. 3601-3623.

**Rots, J. G.** (2001): Sequentially linear continuum model for concrete fracture, in *Fracture Mechanics of Concrete Structures - FRAMCOS4*, 831-840, R. de Borst and J. Mazars and G. Pijaudier-Cabot and J. G. M. van Mier eds., France.

**Simo, J. C.; Oliver, J.; Armero, F.** (1993): An analysis of strong discontinuities induced by strain-softening in rate-dependent inelastic solids, *Computational Mechanics* 12, pp. 277-296.

**Wells, G. N.; Sluys, L. J.** (2000): Analysis of slip planes in three-dimensional solids. *Computer Methods in Applied Mechanics and Engineering* 190 (28), pp. 3591-3606.

